Conformational Changes in Fragments D and Double-D from Human Fibrin(ogen) upon Binding the Peptide Ligand Gly-His-Arg-Pro-Amide[†,‡]

Stephen J. Everse,[§] Glen Spraggon, Leela Veerapandian, and Russell F. Doolittle*

Center for Molecular Genetics University of California, San Diego, La Jolla, California 92093-0634

Received November 4, 1998

ABSTRACT: The structure of fragment double-D from human fibrin has been solved in the presence and absence of the peptide ligands that simulate the two knobs exposed by the removal of fibrinopeptides A and B, respectively. All told, six crystal structures have been determined, three of which are reported here for the first time: namely, fragments D and double-D with the peptide GHRPam alone and double-D in the absence of any peptide ligand. Comparison of the structures has revealed a series of conformational changes that are brought about by the various knob−hole interactions. Of greatest interest is a moveable "flap" of two negatively charged amino acids ($Glu^{\beta 397}$ and $Asp^{\beta 398}$) whose side chains are pinned back to the coiled coil with a calcium atom bridge until GHRPam occupies the β-chain pocket. Additionally, in the absence of the peptide ligand GPRPam, GHRPam binds to the γ-chain pocket, a new calcium-binding site being formed concomitantly.

The principal aim of structural studies on fibrinogen and fibrin is to understand better the details of clot formation. In this regard, it is well-known that fibrin formation is initiated by thrombin cleaving two different arginyl−glycine bonds in each half of the fibrinogen dimer. One of these is near the amino-terminus of the α chain and results in the release of the fibrinopeptide A (16 residues in human). The other is near the amino-terminus of the β-chain and removes the fibrinopeptide B (14 residues in human). The newly exposed sequences on the parent molecule serve as "knobs" that fit into "holes" on neighboring molecules, the ensuing noncovalent interactions being the basis of polymerization. Ordinarily fibrinopeptide A is released much faster than fibrinopeptide B, and it has been supposed that some conformational change or general rearrangement resulting from the first set of knob−hole engagements facilitates the removal of the B peptide (*1*−*3*). There is also a large body of circumstantial evidence that the first interaction, involving the A-knob and a hole on the γ-chain carboxyl domain, leads to the linear growth of a two-molecule thick oligomer with a half-molecule stagger, whereas the second interaction, involving the B-knob, leads to lateral growth of the fiber (refs *4* and *5*, inter alia).

Synthetic peptides patterned on the two knob sequences bind preferentially at two different sites on fibrinogen, as well as on the 86 k Da core fragment D generated from fibrinogen by limited proteolysis, although some weak binding to each other's site is apparent in either case (*6*, *7*). The Gly-Pro-Arg-type peptides (A-knobs) have several attributes absent in the Gly-His-Arg type (B-knobs), however, including the ability to inhibit fibrin formation (*6*, *7*) and use in affinity chromatography for the purification of fibrinogen or fragment D (*8*).

Recently, we reported X-ray structures for fragment D from human fibrinogen and also its factor XIII-cross-linked equivalent, double-D from fibrin (*9*). In the case of double-D, the material was cocrystallized with the ligand GPRPam[1] and, more recently, with both GPRPam and GHRPam together (*10*). Additionally, other workers have reported a structure of a 30 k Da γ-chain carboxyl domain complexed with GPRP (*11*). Previously, the principal focus has been mostly on the nature of ligand attachment, although in the cases of the GPRP and GPRPam reports, modest conformational changes in the binding pocket were noted between the ligated and unligated structures.

We have now determined three additional structures in this series: fragments D and double-D with only the peptide GHRPam present (fD-GH and DD-GH), and double-D with no ligand at all (DD-NL). Comparison of the four double-D structures, each of which is composed of two molecules of cross-linked fragment D and therefore two of each kind of site, has revealed a dramatic conformational change involving a two-residue flap movement in the formation of the β-chain hole that binds GHR-knobs. Additionally, GHRPam in the absence of GPRPam has been found to occupy the γ-chain site, concomitant with the formation of a new calcium-binding site.

[†] This work was supported by Grant HL-26873 from the National Heart, Lung & Blood Institute.

[‡] Atomic coordinates are available from the Brookhaven Protein Data Bank under the access codes 1FZE (DD-NL), 1FZF (DD-GH), and 1FZG (fD-GH).

* To whom correspondence should be addressed. Tel: (619) 534-4417. Fax: (619) 534-4985. E-mail: rdoolittle@ucsd.edu.

[§] Current address: Department of Biochemistry, University of Vermont, Burlington VT.

[1] Abbreviations: GPRPam, Gly-Pro-Arg-Pro-amide; GHRPam, Gly-His-Arg-Pro-amide; DD-NL, double-D no ligands; DD-GP, double-D complexed with GPRPam; DD-GH, double-D complexed with GHRPam; DD-BOTH, double-D complexed with GPRPam and GHRPam; fD-NL, fragment D no ligands; fD-GH, fragment D complexed with GHRPam; LSQ, least squares.

10.1021/bi982626w CCC: $18.00
Published on Web 02/18/1999

MATERIALS AND METHODS

Synthetic peptides were made by the BOC procedure (*12*) on a Beckman model 990 Synthesizer. Fibrinogen was purified from plasma obtained from the San Diego Blood Bank. The factor XIII-cross-linked fragment D (double-D) was prepared according to our previously described procedure (*9*). Crystals were obtained by vapor diffusion from sitting drops at room temperature as described previously (*9, 10, 13*). For DD-NL, 10 mg of fragment double-D/mL in 50 mM Tris buffer, pH 7.0, and 5 mM $CaCl_2$ were mixed in equal volumes (5 mL + 5 mL) with well solution containing 50 mM Tris, pH 8.75, 60 mM $CaCl_2$, 12% PEG 3350, and 2 mM sodium azide. Crystals appeared sporadically and were used to streak-seed new virginal solutions; the seeding reproducibly yielded good crystals. The conditions for streak-seeding differed from the conditions described above only in that the final protein concentration was reduced to 2.5 mg/mL. For DD-GH and fD-GH crystals, the starting solutions also contained 10 mg/mL protein and 10 mM GHRPam; the well solutions contained 50 mM Tris, pH 8.0, 10 or 20 mM $CaCl_2$, 12% PEG 3350, and 2 mM sodium azide. In this regard, in two recent articles from this laboratory (*9, 10*) the concentrations of peptides and calcium were mistakenly reported for the particular DD crystals that were actually described. They were 5 mM peptide and 12.5 mM $CaCl_2$, respectively, and not 2.5 and 7.5 mM. (See correction, Everse et al. (1998) *Biochemistry 37*, 18128.)

Diffraction data from DD-NL and fD-GH crystals were collected at Brookhaven National Synchrotron Light Source, beamline X12C. In the case of DD-NL, a single crystal was flash-frozen in a loop containing 12% PEG 3350 and 20% glycerol. The data for fD-GH were taken from a single crystal at room temperature. Data from several DD-GH crystals were collected at room temperature at Stanford Synchrotron Radiation Laboratory (SSRL), beamline 7-1. In all cases, diffraction data were processed with DENZO and ScalePack (*14*).

Structure Determinations. The unit cell for DD-NL (no ligand) was indistinguishable from that determined for fragment D from human fibrinogen in the absence of ligands (*13*), and as a result, it was possible to use rigid-body refinement (*15*). In contrast, the DD-GH crystals were of a different space group ($P2_12_12_1$), and it was necessary to use molecular replacement (*15)*. In this regard, a rotation search was carried out with one of the unit molecules from DD-BOTH (*10*) with all data in the resolution range 8−4 Å. As in the case of double-D with the ligand GPRPam (*9*), two solutions were obtained that were approximately 180° apart. The correlation coefficients were 29.7 and 36.4%, respectively, and the corresponding *R*-factors 0.527 and 0.522. The solutions were 4.8 and 7.9 σ above the mean, respectively. When both solutions were taken together, the correlation coefficient rose to 60.8% and the *R*-factor dropped to 0.397. From this point on, all data between 30 and 3.0 Å were used. SigmaA-weighted electron density maps were constructed, and the ligand was clearly evident in both $2|F_o - F_c|$ and $|F_o - F_c|$ maps. Crystals of fD-GH had the same space group and unit cell dimensions as DD-GH, and it was possible to obtain the structure by rigid-body refinement (*15*).

Models were improved by cycles of manual fitting with O (*16*) and refinement, including in some cases procedures from X-PLOR (*15*) and in others RefMac from the CCP4 package (*17*). Both the working *R*-factor and free *R*-factor (*18*) were followed closely (Table 1). Extensive use was made of the LSQ superposition operation in O (*16*) for the comparisons of the various structures.

Table 1: Data Collection and Refinement Statistics

	DD-NL	DD-GH	fD-GH
data statistics			
beam	BNL X12C	SSRL 7-1	BNL X12C
detector	Brandeis CCD	Mar	Brandeis CCD
space group	$P2_1$	$P2_12_12_1$	$P2_12_12_1$
unit cell dimensions			
a	108.0	54.8	54.7
b	48.6	149.4	149.5
c	166.4	234.7	232.5
β	104.41		
molecules/asym. unit	1	1	2
number of crystals	1	4	1
resolution (Å)	3.0	2.7	2.5
observations (*N*)	413 251	232 395	737 489
unique reflections (*N*)	35 615	49 458	66 513
mean redundancy	11.6	4.7	11.1
completeness (%)	96.7	88.5	96.0
R_{merge} (*I*) (%)[a]	10.4	11.9	11.1
refinement statistics			
resolution range (Å)	30.0−3.0	30.0−2.7	30.0−2.5
no. of model atoms	11 207	10 585	10 704
R-value[b]	0.251	0.233	0.208
free *R*-value[c]	0.318	0.302	0.260
rmsd from ideals			
bond length (Å)	0.007	0.018	0.02
bond angle (deg)	1.4	3.4	3.2
average *B*-value	53.98	49.50	53.56

[a] $R_{merge} = (\sum|I - <I>|)/(\sum|I|)$. [b] Crystallographic *R*-value $(\sum||F_{(Obs)}| - |F_{(Calc)}||)/(\sum|F_{(Obs)}|)$ with 95% of the native data for refinement. [c] Free *R*-value: *R*-value based on 5% of the native data withheld from refinement.

Molecule Assignment and Chain Designations. The abutment of the two cross-linked fragments D in double-D is offset in such a way that the contribution from the two interactants is not reciprocal (*9*). We have arbitrarily denoted molecule A, composed of chains A, B, and C in all our deposited structures, as being the molecule in which $Arg^{\gamma 275}$ is directed toward $Ser^{\gamma 300}$ on the opposing unit, whereas molecule B has $Arg^{\gamma 275}$ directed back to $Tyr^{\gamma 280}$ (of molecule A). When dealing with interactions at or near the interface, it is important to specify which molecule is being described.

As it happens, the crystal packing in all these structures is similar, different unit cells and space groups not withstanding, and molecule B consistently has fewer crystal contacts than molecule A. As a result, the electron density is usually better in molecule A, although different parts of the structures can be favored differently in this regard.

RESULTS

Binding of GHRPam to β-Chain Site. Comparison of two double-D structures without bound GHRPam (DD-GP and DD-NL) with two other structures in which the ligand is present (DD-GH and DD-BOTH) revealed a significant rearrangement of the amino acid side chains participating in binding the peptide. Thus, in the absence of the ligand, the side chains of residues $Glu^{\beta 397}$ and $Asp^{\beta 398}$ are directed toward the coiled coil by way of a calcium ion bridge involving a γ-chain residue ($Glu^{\gamma 132}$); the calcium bridge had been overlooked in our original report (*9*). In all three

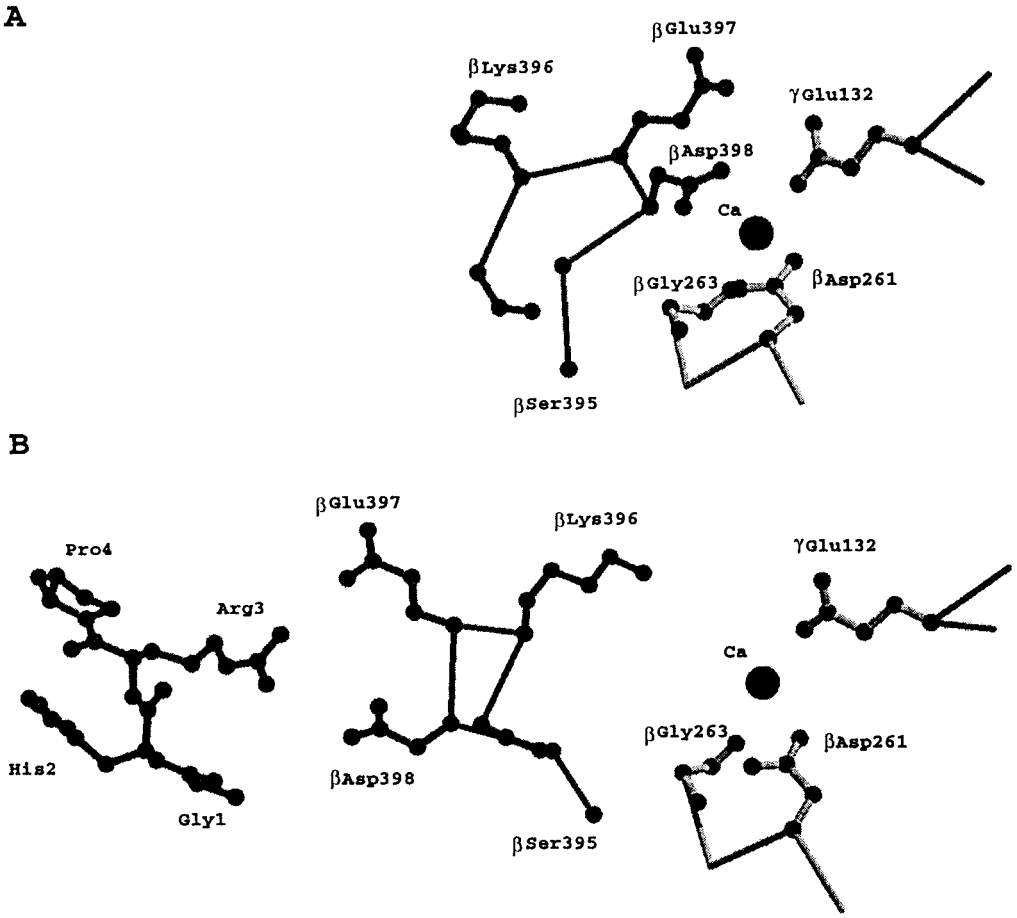

FIGURE 1: Diagrammatic depiction of the conformational change that takes place upon binding of the ligand Gly-His-Arg-Pro-amide (GHRPam) to the β-chain site. The arrangement shown in panel A (upper) occurs in fD-NL, DD-NL, and DD-GP. The arrangement depicted in panel B (lower) occurs in fD-GH, DD-GH and DD-BOTH. Figure prepared with Bobscript (*35, 36)* and Raster3D (*37, 38*).

structures containing the GHRPam ligand (DD-GH, fD-GH, and DD-BOTH), the two side chains have flipped approximately 180°, forming a binding pocket with a similar geometry to the one in the γ-chain carboxyl domain (Figure 1). Both carboxylates are directed toward the guanidino group of Arg-3 in the ligand. The distance moved by the two side-chain carboxylates amounts to about 10 Å. Nonetheless, the calcium bridge is not totally disrupted when the shift occurs. Instead, the lost coordination sites are replaced by the carbonyl oxygen of Gly$^{\beta 263}$ and a water molecule (Figure 1).

Binding of GHRPam to γ-Chain Site. The two structures cocrystallized with only the GHRPam ligand (DD-GH and fD-GH) are isomorphous, and each has the peptide present in both the β- and γ-chain holes. For the most part, the binding interactions appear to be the same as are observed for the ligand GPRPam (Figures 2 and 3). The fact that GHRPam can occupy the site ordinarily occupied by GPRPam prompted us to reexamine our previously reported double-D structure with only the ligand GPRPam (*9*) in which we failed to detect GPRPam in the β-chain hole in the absence of GHRPam. Consistent with there being no peptide present, residues Glu$^{\beta 397}$ and Asp$^{\beta 398}$ in that structure are pointed away from the binding site.

Another New Calcium-Binding Site. Concomitant with the binding of the GHRPam ligand in the γ-chain hole, another calcium ion is bound, the coordination sites of which include the side chains of Asp$^{\gamma 301}$ and Asp$^{\gamma 294}$, and the carbonyl oxygens of Gly$^{\gamma 296}$ and Asp$^{\gamma 298}$ (Figure 4). The involvement of these residues in calcium binding is mainly the result of a shift in the polypeptide backbone in the region including residues Gly$^{\gamma 296}$—Asp$^{\gamma 297}$ (Figure 4).

Larger Scale Differences among the Structures. Possible larger scale changes in the arrangement of the three polypeptide chains, the coiled coils, the carboxyl domains, and the two molecules that comprise the double D, were sought by using the superposition operation (LSQ) of the program O (*16*). Numerous comparisons were conducted that superimposed the corresponding sectors of one of the two unit molecules to see if (a) there was a change in the angle of flexure between the two halves of the double-D molecules or (b) whether there was any change in the relative orientations of the coiled coils. As we noted previously (*10*), the most obvious difference is the change in angle between the abutting molecules. In this regard, DD-GH is "bent" significantly more than the others (Figure 5), the apparent consequence of small changes in interaction near or at the interface, or possibly the result of different crystal contacts in the orthorhombic cell compared with the monoclinic ones. In either case, the differences reflect the looseness of the interfacial contacts in these double-D structures.

DISCUSSION

The initial attack on fibrinogen by thrombin sets in motion a complex and extensive train of events that culminates in the formation of an infinitely long, anastomosing polymer

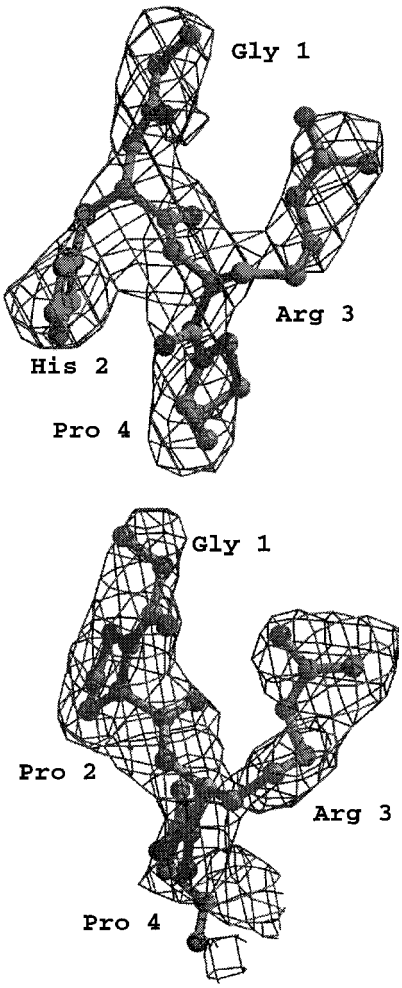

FIGURE 2: Electron density omit maps showing (upper) ligand Gly-His-Arg-Pro-amide (GHRPam) bound to γ-chain binding site in DD-GH compared with (lower) Gly-Pro-Arg-Pro-amide bound to same site in DD-GP. Densities were calculated from $|F_o| - |F_c|$ coefficients and phases from refined model contoured at 2.2 σ. The ligand models were not included in the Fc calculations. Figure prepared with Bobscript (*35, 36)* and Raster3D (*37, 38*).

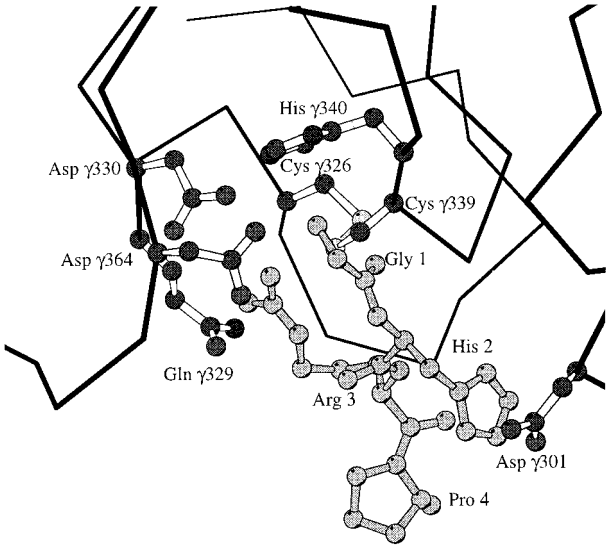

FIGURE 3: Ball and stick diagram of GHRPam (light shading) bound in the γ-chain hole (dark shading). Figure prepared with Bobscript (*35, 36*).

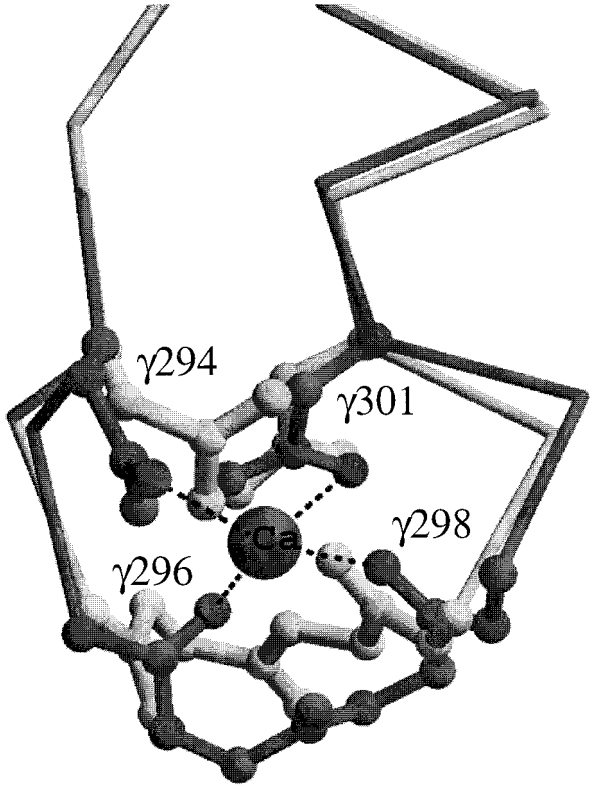

FIGURE 4: Diagram of calcium binding by segment of γ-chain including residues 294−301 in DD-GH (dark gray) compared with DD-BOTH (light gray), which does not have calcium at this site. Note different positions of backbone in the two structures and the participation of the carbonyl oxygen of Gly$^{\gamma 296}$ in ligating calcium in DD-GH. Figure prepared with Bobscript (*35, 36)* and Raster3D (*37, 38*).

which is hundreds of molecules thick. Only some of those events can be reconstructed with proteolytic fragments from fibrinogen and fibrin in conjunction with synthetic peptides. Nonetheless, the experiments presented here are in harmony with past biochemical results and allow a working scenario of certain events to be depicted.

Foremost among the new findings is that the binding site for the B-knob is not fully formed until the knob itself is present, a dramatic conformational change occurring in the presence of the ligand. No such change is observed when GPRPam binds to the γ-chain hole, the participating ligand-binding groups already being correctly positioned. The change in the β-chain site takes the form of a sprung mouse trap in that two critical side-chain carboxylate groups are initially coordinated to a calcium ion pointing away from the pocket. Formation of the pocket deforms but does not completely disrupt the calcium-bridge between the coiled coil and the β-chain carboxyl domain, a new coordination site being provided by a nearby carbonyl oxygen (Figure 1).

It might have been expected that the excursion of residues Glu$^{\beta 397}$ and Asp$^{\beta 398}$ could trigger other rearrangements, perhaps involving movement of the nearby part of the α chain which forms a helix running in the opposite direction to the coiled coil. In this regard, there have been reports that the α-chain carboxyl domain is involved in the lateral association of protofibrils (*19*) and that these interactions occur following a conformational change dependent on the release of fibrinopeptides B (*20*). No such large-scale movement of either the fourth helix or the coiled coil away from the β-chain carboxyl domain or each other was observed, however. It

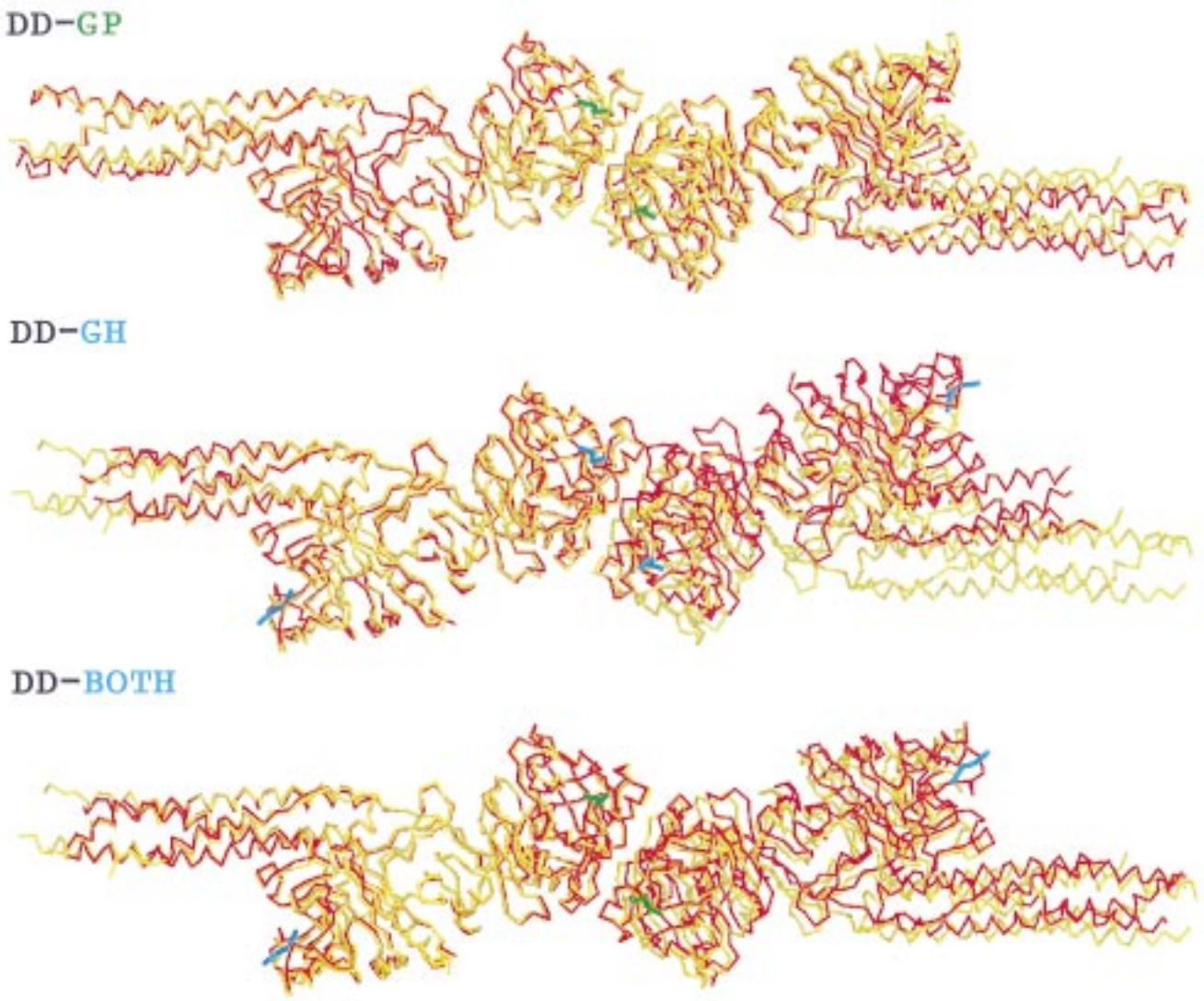

FIGURE 5: Superimposed α-carbon backbone structures of three liganded double-D structures (DD-GP, DD-GH, and DD-BOTH, all colored red) with that of DD-NL (no ligand, colored yellow). The structures were superimposed by setting the γ-chain domains of the molecules A (chains ABC) to coincide. Ligands are colored blue. Note the increased angle between the two halves of DD-GH.

Table 2. Residues Involved in Four Different Calcium-Binding Sites in the Fragment D Portion of Human Fibrinogen

site 1 (strong)[a]	site 2 (weak)[b]	site 3A (weak)[c]	site 3B (weak)	site 4 (weak)[d]
Asp$^{\gamma 318}$ (sc)[e]	Asp$^{\beta 381}$ (sc)	Glu$^{\gamma 132}$ (sc)	Glu$^{\gamma 132}$ (sc)	Asp$^{\gamma 294}$ (sc)
Asp$^{\gamma 320}$ (sc)	Asp$^{\beta 383}$ (sc)	Asp$^{\beta 261}$ (sc)	Asp$^{\beta 261}$ (sc)	Gly$^{\gamma 296}$ (bb)
Phe$^{\gamma 322}$ (bb)[f]	Trp$^{\beta 385}$ (bb)	Glu$^{\beta 397}$ (sc)	Gly$^{\beta 263}$ (bb)	Asp$^{\gamma 298}$ (bb)
Gly$^{\gamma 324}$ (sc)		Asp$^{\beta 398}$ (sc)		Asp$^{\gamma 301}$ (sc)

[a] As first reported by Yee et al. (*29*). [b] From Everse et al. (*10*). [c] Site 3A is converted to 3B upon binding of GHRPam to β-chain pocket. [d] Site 4 occurs only upon binding of GHRPam to γ-chain pocket. [e] sc = sidechain carboxylate. [f] bb = backbone carbonyl.

must be kept in mind, as we have remarked before (*9*), that we are dealing with proteolytic fragments of the fibrin system that may have retreated to their initial positions after proteolysis.

Significance for β-Fibrin. That the GHRPam ligand can occupy the γ-chain hole may offer at least a partial explanation of the enigma of β-fibrin. β-Fibrin is formed by removal of the fibrinopeptide B alone. It can be obtained in some cases by the use of heterologous thrombin (*21*−*23*) and in others by certain snake venoms (*24*−*27*). The fibers and clots of β-fibrin appear similar to those of ordinary fibrin (*24*−*27*). The question has always been, does the B-knob in these situations fit into the β-chain, γ-chain site, or both? Now it is certain that at least the synthetic peptide can indeed bind to both sites when the A-knob is absent. Equilibrium dialysis studies had shown a similar result (*6*, *7*). Although it can be argued that the situation is kinetically controlled—because under physiological conditions the B-knobs are not exposed until the γ-chain sites are mostly filled anyway—the fact that GHRPam does not occupy the γ-chain site when GPRPam is present (*10*) shows that the matter of relative affinities is also a factor.

Calcium Involvements. It is well established that fragment D from human fibrinogen has a single high-affinity calcium-binding site (*28*, *29*) situated on the γ-chain (*30*), although there is evidence for numerous weaker binding sites (*31*),

Table 3. Comparisons of Unit Cells and Space Groups for Six Different Structures of Fragments D and Double-D

	fD-NL	DD-NL	DD-GP	DD-BOTH	DD-GH	fD-GH
space group	$P2_1$	$P2_1$	$P2_1$	$P2_1$	$P2_12_12_1$	$P2_12_12_1$
unit cell						
a	107.7	108.0	93.8	83.4	54.8	54.7
b	48.1	48.6	95.5	95.6	149.4	149.5
c	167.1	166.4	113.8	113.6	234.7	232.9
β	105.7	104.6	96.1	90.2		
temperature	RT	100 K	RT	100 K	RT	RT
molecules/a.u.	2	1	1	1	1	2
[$CaCl_2$] (mM)	25−65	32.5	12.5	12.5	7.5	12.5

also. Recently, we showed that one of these weaker binding sites occurs at a position in the β-chain homologous to the γ-chain high-affinity site (*10*). Now we have identified two more weak binding sites in different parts of the β− and γ-chains (Table 2). Even though calcium is better known for its effects in the later stages of fibrin formation involving the lateral association of protofibrils (*32*, *33*), the involvement of calcium at sites associated with the binding of GHRPam illustrates the complexity of calcium effects in fibrin formation. It should be noted that a direct correlation has been made of the binding of calcium upon release of fibrinopeptide B (*34*, *35*). At this point, however, it is impossible to know if the binding of calcium in conjunction with the binding of GHRPam at the new γ-chain site is merely fortuitous or has some function.

Influence of Ligands on Crystallization. As implied in the Materials and Methods section, the presence or absence of ligand has a direct bearing on the concentration of calcium that will best lead to crystals of fragments D or double-D. Indeed, in the absence of the peptide ligands, we have not yet been able to obtain crystals of double-D at calcium concentrations lower than 30 mM, whereas in the presence of the peptide ligands, crystallization does not easily occur much above 15 mM calcium.

It is noteworthy, also, that the particular ligand employed has a direct bearing on the mode of crystallization with regard to space group and unit cell dimensions (Table 3). Moreover, the fragment D crystals usually form the same end-to-end packing arrangement as is found in crystals of the cross-linked double-D molecules. Thus, fD−GH is isomorphous with DD−GH, and fD−NL is isomorphous with DD-NL. The exception is the complex of GPRPam with fragment D, which crystallizes in a different space group and unit cell from DD-GP (*13*). The very large unit cell of the fD−GP complex, combined with a large degree of mosaicity, has been a hindrance to obtaining a structure. Crystals of the complex fD−BOTH have also been unsatisfactory so far. Whether these problems are mere happenstance or reflect some important change when fD binds the GPRPam ligand remains to be determined.

REFERENCES

1. Blomback, B., Hessel, B., Hogg, D., and Therkildsen, L. (1978) *Nature 275*, 501−505.
2. Hantgan, R. R., and Hermans, J. (1979) *J. Biol. Chem. 254*, 11272−11281.
3. Hurlet-Jensen, A., Cummins, H. Z., Nossel, H. L., and Liu, C. Y. (1982) *Thromb. Res. 27*, 419−427.
4. Laurent, T. C., and Blomback, B. (1958) *Acta Chem. Scand. 12*, 1875−1977.
5. Weisel, J. W., Veklich, Y., and Gorkun, O. (1993) *J. Mol. Biol. 232*, 285−297.
6. Laudano, A. P., and Doolittle, R. F. (1978) *Proc. Natl. Acad. Sci. U.S.A. 75*, 3085−3089.
7. Laudano, A. P., and Doolittle, R. F. (1980) *Biochemistry 19*, 1013−1019.
8. Kuyas, C., Haeberli, A., Walder, P., and Straub, P. W. (1990) *Thromb. Haemost. 63*, 439−444.
9. Spraggon, G., Everse, S. J., and Doolittle, R. F. (1997) *Nature 389*, 455−462.
10. Everse, S. J., Spraggon, G., Veerapandian, L., Riley, M., and Doolittle, R. F. (1998) *Biochemistry 37*, 8637−8642.
11. Pratt, K. P., Cote, H. C. F., Chung, D. W., Stenkamp, R. E., and Davie, E. W. (1997) *Proc. Natl. Acad. Sci. U.S.A. 94*, 7176−7181.
12. Merrifield, R. B. (1964) *Biochemistry 3*, 1385−1390.
13. Everse, S. J., Pelletier, H., and Doolittle, R. F. (1995) *Protein Sci. 4*, 1013−1016.
14. Otwinowski, Z., and Minor, W. (1997) *Methods Enzymol. 276*, 307−326.
15. Brunger, A. T. X-PLOR. Version 3.1. A System for X-ray Crystallography and NMR. Yale University Press, New Haven, 1992.
16. Jones, T. A., Zou, J.-Y, Cowan, S. W., and Kjeldgaard, M. (1991) *Acta Crystallogr., Sect. A 47*, 110−119.
17. Collaborative Computing Project Number 4 (1994) The CCP4 suite: Programs for protein crystallography, Version 3.1, *Acta Crystallogr., Sect. D* 50, 760−763.
18. Brunger, A. T. (1992) *Nature 355*, 472−475.
19. Veklich, Y. I., Gorkun, O. V., Medved, L. V., Nieuwenhuizen, W., and Weisel, J. W. (1993) *J. Biol. Chem. 268*, 13577−13585.
20. Gorkun, O. V., Veklich, Y. I., Medved, L. V., Henschen, A. H., and Weisel, J. W. (1994) *Biochemistry 33*, 6986−6997.
21. Doolittle, R. F. (1965) *Biochem. J. 94*, 735−741.
22. Doolittle, R. F.; Cottrell (1976) *Biochim. Biophys. Acta 453*, 426−438.
23. Doolittle, R. F. (1991) In *Fibrinogen, Thrombosis, Coagulation and Fibrinolysis* (Liu, C. Y., and Chien, S., Eds.) pp 25−37 Plenum Press, New York. 1991.
24. Shainoff, J. R., and Dardik, B. N. (1979) *Science 204*, 200−202.
25. Weisel, J. W. (1986) *Biophys. J. 50*, 1079−1093.
26. Dyr, J. E., Blomback, B., Hessel, B., and Kornalik, F. (1989) *Biochim. Biophys. Acta 990*, 18−24.
27. Marguerie, G., Chagniel, G., and Suscillon, M. (1977) *Biochim. Biophys. Acta 490*, 94−103.
28. Haverkate, F., and Timan, G. (1977) *Thromb. Res. 10*, 803−812.
29. Yee, V. C., Pratt, K. P., Cote, H. C., LeTrong, I., Chung, D. W., Davie, E. W., Stenkamp, R. E., and Teller, D. C. (1997) *Structure 5*, 125−138.
30. Van Ruijven-Vermeer, I. A. M., Nieuwenhuizen, W., and Nooijen, W. J. (1978) *FEBS Lett. 93*, 177−180.
31. Boyer, M. H., Shainoff, J. R., and Ratnoff, O. D. (1972) *Blood 39*, 382−387.
32. Marx, G. (1987) *Biopolymers 26*, 911−920.
33. Mihalyi, E. (1988) *Biochemistry 27*, 967−976.
34. Mihalyi, E. (1988) *Biochemistry 27*, 976−982.
35. Kraulis, P. J. (1991) *J. Appl. Crystallogr. 24*, 946−950.
36. Esnouf, R. M. (1997) *J. Mol. Graphics 15*, 133−138.
37. Bacon, D. J., and Anderson, W. F. (1988) *J. Mol. Graphics 6*, 219−220.
38. Merritt, E. A., and Murphy, M. E. P. (1994) *Acta Crystallogr., Sect. D 50*, 869−873.

BI982626W